Ultrasound-Assisted Synthesis of Defective MOF-801 for the Adsorptive Removal of Cationic Dyes

Penmethsa, Kiran Kumar; Sunkara, Satya Veni*[+]

Department of Chemistry, Jawaharlal Nehru Technological University Kakinada (JNTUK) Kakinada-533003, Andhra Pradesh, INDIA

ABSTRACT: *Defective MOF-801 (Zirconium-fumarate metal-organic framework) was de novo synthesized using environmentally friendly ultrasound-assisted synthesis. The effect of the modulator on the crystallinity, morphology, density of missing linkers, pore volume, and the specific surface area (BET) of synthesized MOF-801 was studied using two modulators, acetic acid, and formic acid, in different quantities. The MOF-801 sample (MOF-801-100FA) was applied to investigate the adsorptive removal of two cationic dyes viz Crystal Violet (CV) and Methylene Blue (MB) from an aqueous solution in a single system. MOF-801-100FA was found to be more effective in removing MB dye than CV dye. The maximum equilibrium adsorption capacity was 30.4 mg/g and 18.9 mg/g with MB and CV dyes having an initial concentration of 50 mg/L. Langmuir and Freundlich isotherm models were the best fit for adsorption data based on linear regression analysis. The best kinetic model for the adsorption was pseudo-second-order kinetics (R^2 = 0.9975 for CV dye and 0.9998 for MB dye). The effect of dye concentration, contact time, MOF dose, and pH of dye solution on the adsorption of dyes was also investigated. The study showed that defective MOF-801-100FA is an efficient adsorbent for the removal of CV and MB dyes from aqueous solution*.

KEYWORDS: *MOF-801; Ultrasound-assisted; Cationic dyes; Crystal violet; Methylene blue; Adsorptive removal.*

INTRODUCTION

Dyes are widely used in paper, pharmaceutical, printing, food, textile, and plastic industries. During the dyeing process, lakhs of tons of dyes are lost to effluents. Dye-containing wastewater is harmful to the environment and threatens human and animal health. Therefore, removing the dyes from wastewater before releasing them into the water stream is an essential and challenging task. Although several methods are good at removing dyes from contaminated water, adsorptive removal is one of the best options due to ease of operation, high performance, and low cost of application. Many adsorbents were used for the adsorptive removal of dyes [1-5]. MOFs are employed for the removal of these dyes from aqueous solutions as they possess unique characteristics compared to conventional adsorbents [6-8].

**To whom correspondence should be addressed.*

+ E-mail: dr.satyapurna@gmail.com

1021-9986/2023/10/3293-3305 13/$/6.03

Metal-Organic Frameworks (MOFs) are porous coordination polymers having three-dimensional network structures constructed by coordination-driven self-assembly of inorganic polynuclear clusters known as secondary building units (SBUs) and multitopic organic linkers. The modulator synthesis strategy is used for the synthesis of crystalline MOFs as in the absence of a modulator, mostly amorphous MOF is obtained. Usually, the synthesis of MOF takes place using higher amounts of monotopic acids as modulators which compete with linkers for the coordination of metal ions. It is well-known that a higher concentration of modulators induces structural defects in MOFs. The density of structural defects depends on the nature and concentration of the modulator used in the synthesis. Many of the synthesized MOFs are known to have structural defects. The study of structural defects is of paramount importance as they influence the properties of MOFs [9-12].

MOF-801 is one of the most widely studied metal-organic frameworks. It has exceptional hydrothermal stability. It is the smallest member of Zirconium-based metal-organic frameworks first reported by *Wißmann et al*., (2012) [13]. It is one of the commercially available Zirconium MOFs. Many potential applications of MOF-801 were reported in the literature. It was used in hydrogen and water storage [14], water harvesting from the air [15], photocatalytic degradation of methyl violet 2B [16], removal of fluoride [17], arsenite, and arsenate [18], Chromium (VI) ions [19, 20], nanoscale drug delivery [21], and separation of propylene/propane mixture [22].

Compared to traditional energy sources, ultrasound provides unusual reaction conditions wherein very high temperatures and pressure are generated quickly due to cavitation. There are several reports in the literature about the application of ultrasound irradiation for a large variety of syntheses [23-25]. Soon after the first ultrasound-assisted synthesis of MOFs reported by *Qiu et al*., (2008) [26], many reports were published in the literature about the successful preparation of nano/microporous MOFs. Only a few reports in the literature describe the ultrasonic-assisted synthesis of Zirconium-based MOFs [16, 27]

In the present study, a series of four defective MOF-801 samples were *de novo* synthesized using rapid and environmentally friendly ultrasonic-assisted synthesis. The *de novo* synthesized MOF samples were characterized by various characterization methods and their specific surface area (BET) values were determined. The role of two modulators on the density of missing linkers in the synthesized MOFs was analyzed based on the ThermoGravimetric Analysis (TGA) plots. It was found that the defective MOF-801-100FA carries a negative charge at basic pH and hence can accommodate the cationic dyes. The cationic dyes, MB and CV, possessing positive charge are selectively adsorbed through electrostatic interactions by MOF-801-100FA with a negative charge. The presence of these cationic dyes in aqueous solution is not desirable as they are biohazard substances, and potentially carcinogenic materials [28, 29]. The adsorptive removal of these dyes by defective MOF-801-100FA was investigated in detail using different adsorption isotherms and kinetic models.

EXPERIMENTAL SECTION

Materials and equipment

All the chemicals purchased from Sigma Aldrich were used as such without purification. Powder X-Ray Diffraction (PXRD) patterns were recorded using monochromatized Cu Kα radiation (λ = 1.5406 Å) on a Bruker D8 Advance diffractometer operated at 40 kV and 40 mA. Field-Emission Scanning Electron Microscopy (FE-SEM) images were obtained on a Supra55 Zeiss instrument. Scanning Electron Microscopy- Energy Dispersive X-ray spectroscopy (SEM-EDX) was recorded at 10 kV acceleration voltage to determine the elemental composition of MOF samples. The Fourier transform infrared (FT-IR) spectra were recorded on an Agilent Cary 660 instrument in the transmission mode (in the 400 cm^{-1} - 4000 cm^{-1} range). ThermoGravimetric Analysis (TGA) measurement was recorded in the air using Perkin Elmer STA 6000 thermal analyzer. Specific surface area (BET) values are obtained from Nitrogen adsorption-desorption isotherms recorded using a BELSORP analyzer at -196 °C. ANM USC 300 Ultrasonic bath was used for ultrasonication. The absorbance of dye solutions in the visible region was determined using a Shimadzu UV-2450 spectrophotometer. The pH of the dye solutions was altered using 0.1 M HCl and 0.1 M NaOH solutions. A digital pH meter (Model 335, Systronics) was used to determine the pH of the solutions.

Synthesis of defective MOF-801 samples

A series of four defective MOF-801 samples were synthesized under optimum reaction conditions at room temperature

Table 1: Optimum reaction conditions for the synthesis of defective MOF-801 samples using ultrasonication

MOF sample	$ZrOCl_2.8H_2O$ (mmol)	Fumaric acid (mmol)	Acetic acid(mL)	Formic acid (mL)	DMF (mL)	Time(h)
MOF-801-70FA	1.5	1.5	0	4.2	12	4
MOF-801-100FA	1.5	1.5	0	6.0	12	4
MOF-801-70AA	1.0	1.0	4.2	0	8	4
MOF-801-100AA	1.0	1.0	6.0	0	8	4

using different amounts of formic acid/ acetic acid modulators as presented in Table 1. MOF-801 samples synthesized with 70 and 100 equivalents of acetic acid with respect to the $ZrOCl_2.8H_2O$ (metal precursor) were named MOF-801-70AA and MOF-801-100AA respectively and with 70 and 100 equivalents of formic acid were named MOF-801-70FA and MOF-801-100FA respectively.

$ZrOCl_2.8H_2O$ was dissolved in DMF, then fumaric acid was added to the solution. After that respective amount of formic acid/acetic acid was added. The reaction mixture was placed in the ultrasonic bath for 4 hours. Ultrasonic irradiation having a frequency of 40 kHz with a power of 150 watts was applied at room temperature. The temperature of the reaction mixture during sonication was monitored and was found to be less than 60 °C even after the reaction time of 4h. The synthesis of MOF-801-100FA was outlined in Scheme 1.

After cooling down to room temperature, the as-synthesized white crystalline MOFs were recovered by filtration. The crystalline materials were washed three times with 10 mL of DMF followed by ethanol (3 x 10 mL) and acetone (3 x 10 mL). The materials were dried overnight at room temperature and then activated by heating at 100 °C under vacuum for 8 h.

Adsorption study

Removal of two cationic dyes, MB, and CV, from single dye solutions by adsorption, was studied using as-synthesized MOF-801-100FA as the adsorbent. The adsorption of MB and CV dyes from aqueous solution in a single system was investigated using the dye solutions having different initial concentrations, varying the pH of dye solutions, taking different MOF doses, and varying the contact time of MOF with the dye solutions. Adsorption studies were carried out at a temperature of 28 ± 2 °C. Standard solutions of the dyes were prepared by dissolving 1000 mg of the dye in 1000 mL of distilled water. A set of standard solutions for each dye was prepared using the stock solutions. The absorbance maximum of dye solutions at 590 nm for CV and 665 nm for MB was measured and calibration curves were plotted for each of the dye solutions. 50 mL of each dye solution in a single system was used to study the adsorption. The dye solution and MOF-801-100FA were mixed using a magnetic stirrer at 300 rpm. The adsorption efficiency, Q_e (mg/g), was calculated using Equation (1):

$$Q_e = \frac{V\,(C_o - C_e)}{M}, \quad (1)$$

Where C_o (mg/L) was the initial dye concentration, and C_e (mg/L) was the dye concentration at equilibrium. V (L) was the volume of the dye solution, and M (g) is the mass of MOF-801-100FA. 20 mg of MOF-801-100FA was added to each of the 50 mL dye solutions having a concentration of 5, 10, 20, 30, 40, and 50 mg/L. After the time interval of 12 hours, the absorbance of each solution was measured and the C_e values were determined from the absorbance values using the calibration curves.

The percentage removal of dyes was calculated using Equation (2):

$$\text{Percentage removal} = \frac{(C_o - C_e)}{C_o} \times 100\%, \quad (2)$$

Adsorption isotherms were described using Freundlich, Langmuir, and Temkin adsorption isotherm models.

Freundlich adsorption isotherm is expressed as Equation (3):

$$\ln Q_e = \ln K_F + \frac{1}{n} \ln C_e \quad (3)$$

Here, K_F is the Freundlich constant, and n is the constant whose value indicates the favourability of the adsorption process.

The value of 1/n provides information about the usability of the adsorbent over the concentration range of the dye solution.

Langmuir isotherm is represented by Equation (4):

$$\frac{C_e}{Q_e} = \frac{C_e}{Q_m} + \frac{1}{Q_m K_L} \quad (4)$$

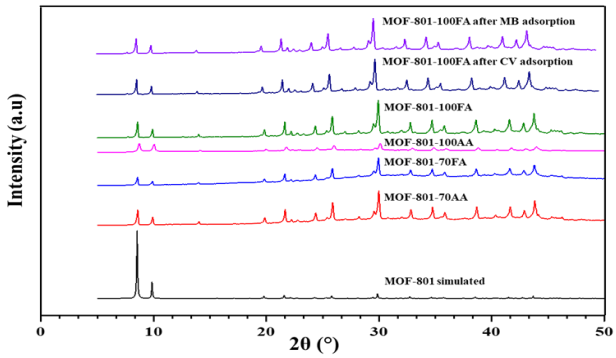

Fig. 1: PXRD patterns of MOF-801 simulated, MOF-801-70AA, MOF-801-70FA, MOF-801-100AA, MOF-801-100FA and MOF-801-100FA after CV adsorption, and MOF-801-100FA after MB adsorption

Here, Q_e is the maximum adsorption capacity (mg/g) of the adsorbent (MOF-801-100FA) with the highest concentration of dye (100 mg/L) used in the adsorption experiment, and K_L is the Langmuir adsorption constant.
Temkin isotherm is given by Equation (5):

$$Q_e = \frac{RT}{B_T} \ln C_e + \frac{RT}{B_T} \ln K_T \quad (5)$$

Here, B_T is the adsorption heat constant (J) and K_T is the equilibrium binding constant (L/ mg)

Adsorption kinetics

For the kinetic study, 50 mL of CV or MB dye solution having a concentration of 5 mg/L and 20 mg of MOF-801-100FA as adsorbent was used. At the desired time (t), the dye solution was withdrawn and the absorbance was measured. Q_t (mg/g), dye amount adsorbed at time t, was obtained by Equation (6):

$$Q_t = \frac{V(C_o - C_t)}{M} \quad (6)$$

Here, C_t (mg/L) is the dye concentration at time t (min).
To study the kinetics in the adsorption process, three kinetic models, pseudo-first-order, pseudo-second-order, and Intraparticle diffusion were used. These three models are expressed as Equations (7), (8), and (9):
Pseudo-first-order kinetics,

$$\ln(Q_e - Q_t) = \ln Q_e + k_1 t \quad (7)$$

Pseudo-second-order kinetics,

$$\frac{t}{Q_t} = \frac{1}{k_2 Q_e^2} + \frac{1}{Q_e} t \quad (8)$$

Intraparticle diffusion kinetics,

$$Q_t = k_i t^{1/2} + C \quad (9)$$

Here, k_1 (min^{-1}), k_2 (g/mg min) and k_i ($mg/g\ min^{1/2}$) are the rate constants for pseudo-first-order, pseudo-second-order, and intraparticle diffusion respectively. C is the intraparticle diffusion constant.

Desorption of MOF

The MB dye and CV dye adsorbed-MOFs were separated from the respective dye solutions by centrifugation (6000 rpm for 20 min). Thereafter, the MOFs were washed with methanol several times until no violet color in the methanol solution while washing the CV-loaded MOF and no blue color in methanol solution while washing the MB-loaded MOF was observed. Finally, the recovered MOFs were activated by drying under vacuum at 100 °C for 8 h. The adsorption-desorption process was performed for five consecutive cycles.

RESULTS AND DISCUSSION

Characterization of defective MOF-801 samples

The as-synthesized crystalline MOFs were characterized using different characterization techniques. The Powder X-Ray Diffraction (PXRD) patterns of the synthesized materials were compared with simulated patterns of MOF-801 in Fig. 1 [30]. The synthesized materials' peaks fit well with the simulated MOF-801. The characteristic peaks positioned around $2\theta = 8.5^o$ and 9.8^o in the PXRD patterns indicate the successful synthesis of MOF-801 samples. The presence of sharp peaks suggests that highly crystalline MOF-801 samples were obtained. The effect of the modulator's type and concentration on the MOF's crystallinity was evident in Fig.1. With the increase in the concentration of the formic acid modulator from 70 equivalents to 100 equivalents, there is an increase in the intensity of the peaks indicating the increase in the crystallinity of the MOF. Such a trend is not observed with the acetic acid modulator. Under identical reaction conditions, the highest crystallinity was observed with 70 equivalents of acetic acid in MOF-801-70AA amongst MOF-801-70AA, and MOF-801-100AA. Among the synthesized MOFs, sharp and high-intensity peaks are observed in MOF-801-100FA. A comparison between PXRD patterns before and after adsorption by MOF-801-100FA indicates that the MOF framework was intact even after the adsorption of CV and MB dyes.

The morphology of the samples was characterized by FE-SEM. The FE-SEM images were presented in Fig. 2. With the increase in the concentration of acetic acid,

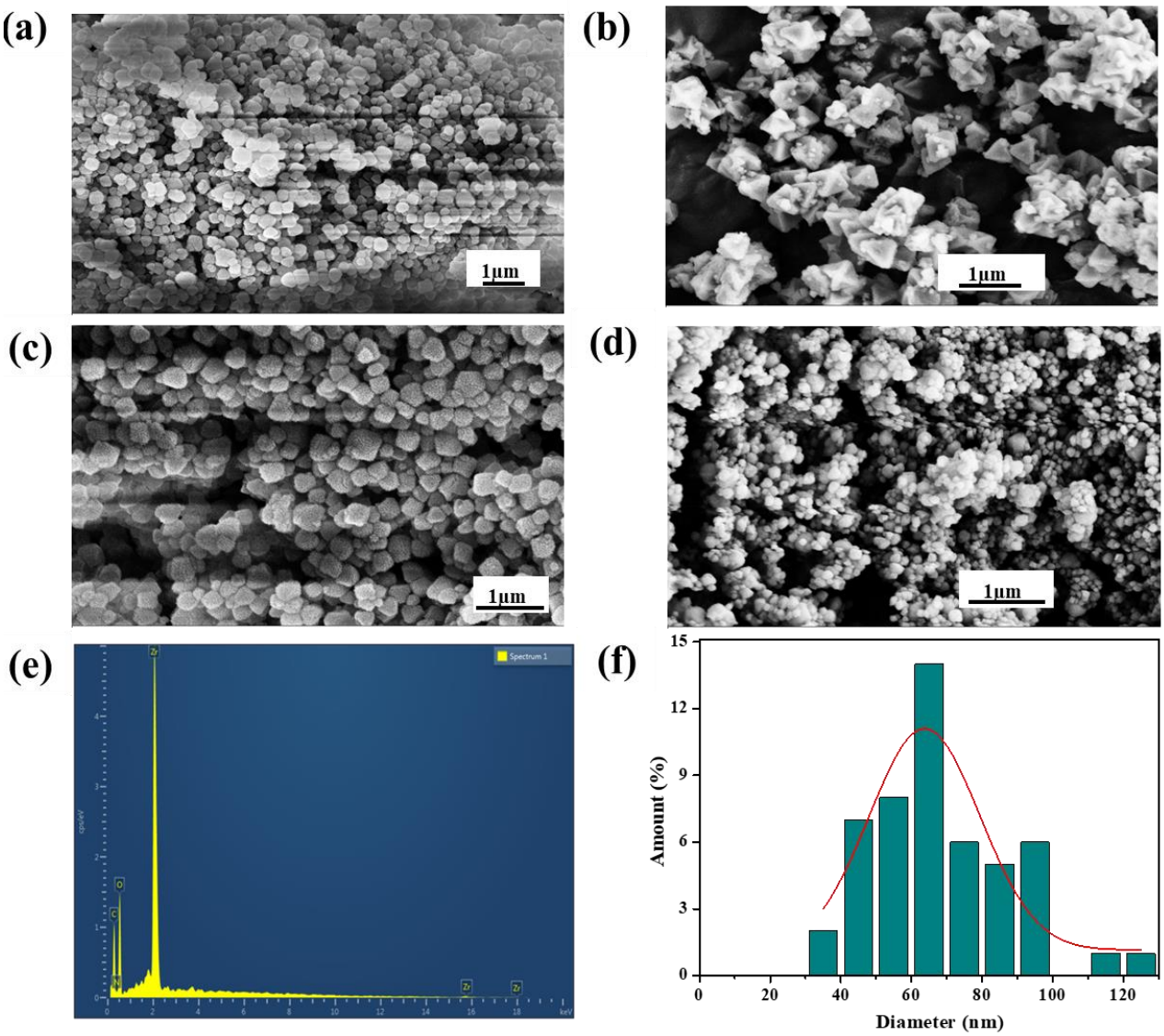

Fig. 2: FE-SEM images of MOF-801-70AA (a), MOF-801-100A (b), MOF-801-70FA (c), MOF-801-100FA (d), SEM-EDX spectrum of MOF-801-100FA (e), and Particle size distribution of MOF-801-100FA particles from SEM images (f)

an increase in the size of the particles was observed. Whereas the particle size decreased with the increase in the concentration of formic acid modulator from 70 to 100 equivalents. The SEM-EDX spectrum of MOF-801-100FA was given in Fig. 2. Zirconium (Lα= 2.042 keV), carbon (kα = 0.277 keV), and oxygen (kα = 0.525 keV) were identified in the spectrum based on the energies of the emitted X-rays from these elements. Particles of MOF-801-100FA are cubic with an average diameter of 68.1 nm as determined from the size of 50 particles using ImageJ. A histogram fitted with Gaussian distribution of the size of the MOF-801-100FA particles was presented in Fig. 2.

The FT-IR spectra of the MOF-801 samples were found in Fig. 3. The bands at 491 cm^{-1} and 660 cm^{-1} could be assigned to the asymmetric stretching vibration of Zr-(OC) and bending vibration of $Zr_6(OH)_4O_4$ cluster respectively. Absorption bands observed at 796 cm^{-1}, 987 cm^{-1}, and 1210 cm^{-1} could be assigned to C-H vibrations. Strong absorption bands observed at 1402 cm^{-1} and 1578 cm^{-1} were ascribed to the symmetrical stretching and asymmetrical stretching vibrations of the carboxylic group of the fumaric acid linker [31].

Nitrogen adsorption-desorption isotherms of activated MOF-801 samples were presented in Fig. 4. All the isotherms

Table 2: Comparison of the specific surface areas determined from N_2 sorption isotherms of MOF-801samples

MOF-801 sample	BET area (m^2/g)	Pore volume (cm^3/g)	Mean pore diameter (Å)
MOF-801-100FA	699	0.31	17.86
MOF-801-70FA	578	0.39	26.8
MOF-801-100AA	224	0.13	23.9
MOF-801-70AA	234	0.20	34.7

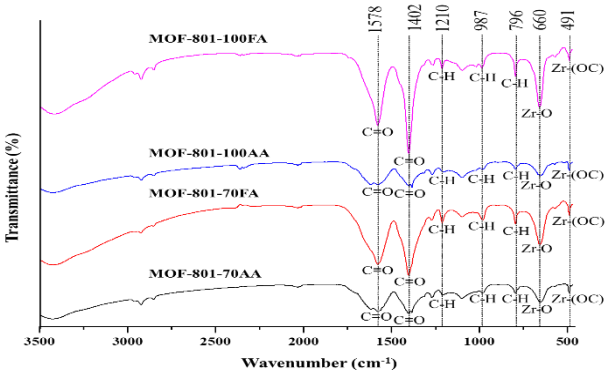

Fig. 3: FT-IR spectra of MOF-801-70AA, MOF-801-70FA, MOF-801-100AA, MOF-801-100FA

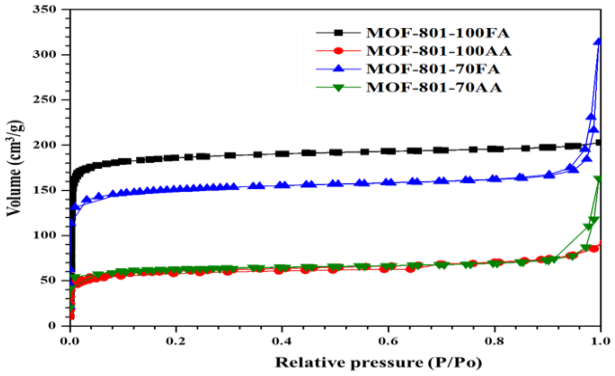

Fig. 4: Nitrogen adsorption-desorption isotherms of MOF-801-70AA, MOF-801-70FA, MOF-801-100AA, and MOF-801-100FA

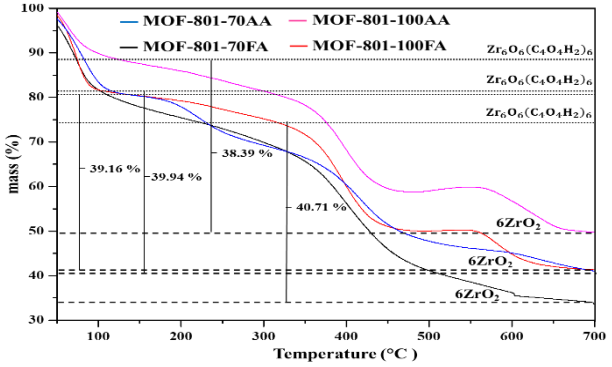

Fig. 5: The TG curves of MOF-801-70AA, MOF-801-70FA, MOF-801-100AA, and MOF-801-100FA

are type-1 based on IUPAC classification. They indicate that the materials are microporous. Among the MOF-801 samples, MOF-801-100FA has the highest specific surface area (BET area) of 699 m^2/g. The BET area, pore volume, and mean pore diameter of the MOF-801 samples were presented in Table 2.

Thermogravimetric analysis curves of the defective MOF-801 samples were presented in Fig. 5. All the synthesized MOFs exhibited almost similar shapes of TGA curves. Either Acetic acid or formic acid modulator has produced no appreciable changes in the shapes of TGA curves. As reported in the literature there are three distinct mass loss steps in the TGA curves [14]. In the first step occurring below 120 °C mass loss was due to the evaporation of water molecules occluded in the pores. The mass loss in the second step occurring at 250-400°C could be attributed to the decomposition of the linker molecules. The last step occurring at around 550-680 °C can be assigned to the decomposition of carboxylate ions coordinated to zirconium cations releasing carbon dioxide. Assuming that the mass loss occurring between 250 and 680 °C is due to the decomposition of the linker, the formation of ZrO_2 as the final product after heating of MOF-801 in the air is given by the following Equation (10):

$$Zr_6O_6(C_4O_4H_2)_6 + 18O_2 \rightarrow 6ZrO_2 + 24CO_2 + 6H_2O \quad (10)$$

Based on the stoichiometry of the Equation, from one formula unit of $Zr_6O_6(C_4O_4H_2)_6$, six moles of ZrO_2 are obtained. Assuming that 100 g of initial $Zr_6O_6(C_4O_4H_2)_6$ was taken, the mass of the solid residue ZrO_2 should be 55.7 g corresponding to a relative mass loss of 44.3%. The recorded mass losses for the MOF samples were below the theoretical value. For MOF-801-70AA, MOF-801-100AA, MOF-801-70FA and MOF-801-100FA the observed mass losses were 39.94%, 38.39%, 40.71% and 39.16% respectively. According to the recent study on defective MOF-801, the deviation of the mass loss from the theoretical value in the region of 250 and 680 °C is proportional to the number of missing linkers in its structure [32].

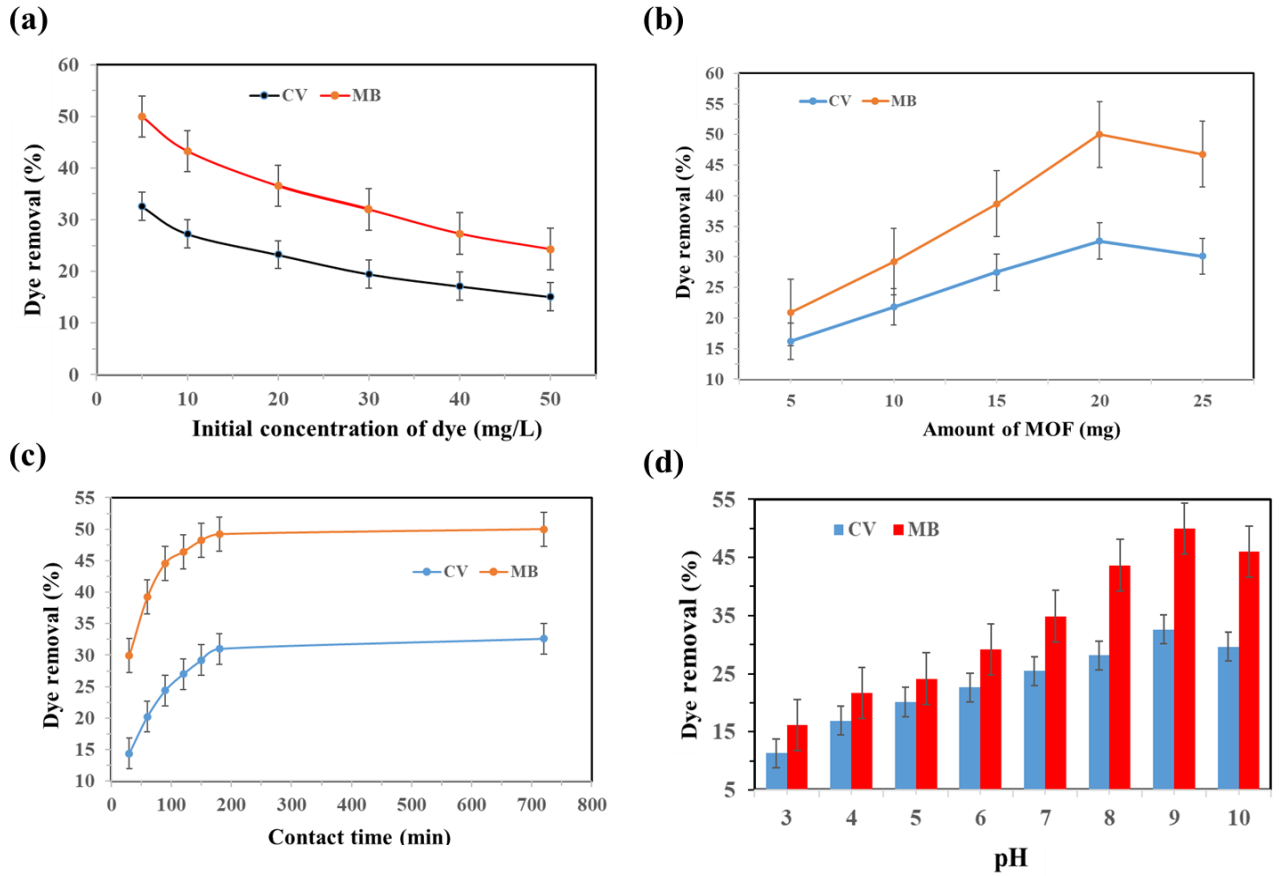

***Fig. 6: Factors affecting the adsorption of CV and MB dyes onto MOF-801-100FA. The initial concentration of dye (a), amount of MOF-801-100FA* (b), *contact time* (c), *and pH of the dye solution* (d)**

Applying the same analogy to the present study suggests that the synthesized MOFs have missing-linker defects. Other reported studies also support our findings that there are missing-linker defects in the *de novo* synthesized MOF-801 frameworks [9, 33]. From the mass loss changes, it is evident that there were significant changes in the density of missing linkers with the amount of acetic acid and formic acid modulators used in the synthesis of MOF-801.

Effect of initial dye concentration

Taking 20 mg of MOF-801-100FA adsorbent, the adsorption experiments were carried out by varying the initial concentration of CV and MB dyes in the range of 5-50 mg/L. The equilibrium time for adsorption was 12h. The effect of the initial concentration of dyes on the adsorption by MOF-801-100FA was shown in Fig. 6(a). The percentage removal of CV dye decreased from 32.6% to 15.10% and MB dye from 50% to 24.32% with an increase in the initial concentration of dye from 5 mg/L to 50 mg/L. As reported in the earlier study, the decrease in the percentage removal of dye can be attributed to the saturation of adsorption sites with the initial dye concentration of 5 mg/L [34].

Effect of MOF-801-100FA dose

The effect of the MOF-801-100FA dose on the percentage removal of CV and MB dyes in the adsorption experiments was shown in Fig. 6(b). Adsorption experiments were conducted by adding a MOF-801-100FA dose of 5,10,15,20, and 25 mg to each 50 mL of 5 mg/L CV and MB dye solutions. Maximum dye removal percentage was achieved with 20 mg of MOF dose as it has a large surface area. The percentage removal of CV dye increased from 16.21% to 32.6% and MB dye increased from 20.9% to 50% with the increase in the dose of MOF-801-100FA from 5 mg to 20 mg.

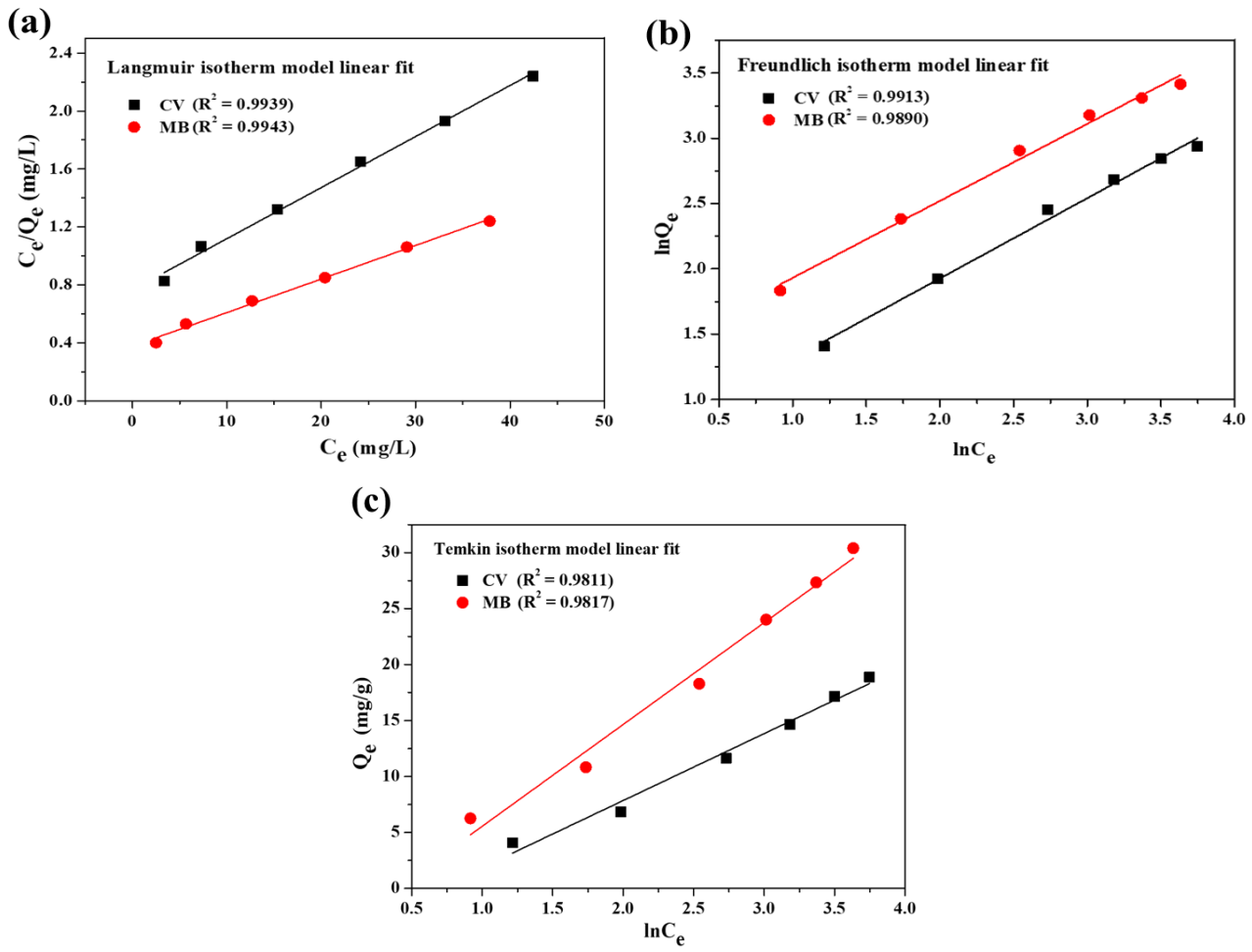

Fig. 7: Plot of linear fitting Langmuir isotherm model (a), Freundlich isotherm model* (b)*, and Temkin isotherm model* (c) *for CV and MB adsorption

Effect of contact time

The effect of contact time on the adsorption of CV and MB dyes was studied by fixing the maximum contact time at 12 hours. The variation in the percentage of dye removal with the contact time was shown in Fig. 6(c). The maximum CV and MB dye removal percentage achieved was found to be 32.6% and 50% respectively. After an initial rise in the percentage of dyes adsorbed onto the MOF-801-100FA surface, there was a slowdown in the percentage of dyes adsorbed with contact time. The extent of adsorption of dyes decreases with an increase in contact time due to the decrease in the number of active sites on the surface of MOF-801-100FA.

Effect of pH

The effect of pH of the dye solutions on the adsorptive removal of dyes by the MOF-801-100FA was studied by performing the adsorption experiments with 50 ml of CV and MB dyes having a concentration of 5 mg/L, and 20 mg of MOF-801-100FA at a temperature of 30 ± 2 °C for a contact time of 12 hours. The change in percentage removal of CV and MB dyes by MOF-801-100FA with the change in the pH of dye solutions from 3.0 to 10.0 was shown in Fig. 6(d). An increase in the percentage removal with the increase in pH of the dye solutions from 3.0 to 9 was observed. Maximum adsorption of dyes was observed at a pH of 9.0. The isoelectric point of MOF was found to be 6.5. Above this pH value, the MOF surface carries a negative charge and readily binds with the cationic dyes, CV and MB, existing in positive form through electrostatic interactions. The possible mechanism for the adsorption of CV and MB dyes by MOF adsorbent is via electrostatic interaction [6, 35].

Table 3: Isotherm parameters for adsorption of CV and MB dyes on MOF-801-100 FA

Dye	$Q_{e,exp}$ (mg/g)	Freundlich isotherm			Langmuir isotherm			Temkin isotherm		
		n	K_F (mg/g)	R^2	Q_m (mg/g)	K_L (L/mg)	R^2	B_T (J)	K_T (L/mg)	R^2
CV	18.88	2.01	0.6991	0.9913	28.37	0.0460	0.9939	421	0.50	0.9811
MB	37.84	1.69	3.83	0.9890	43.14	0.0614	0.9943	277	0.68	0.9817

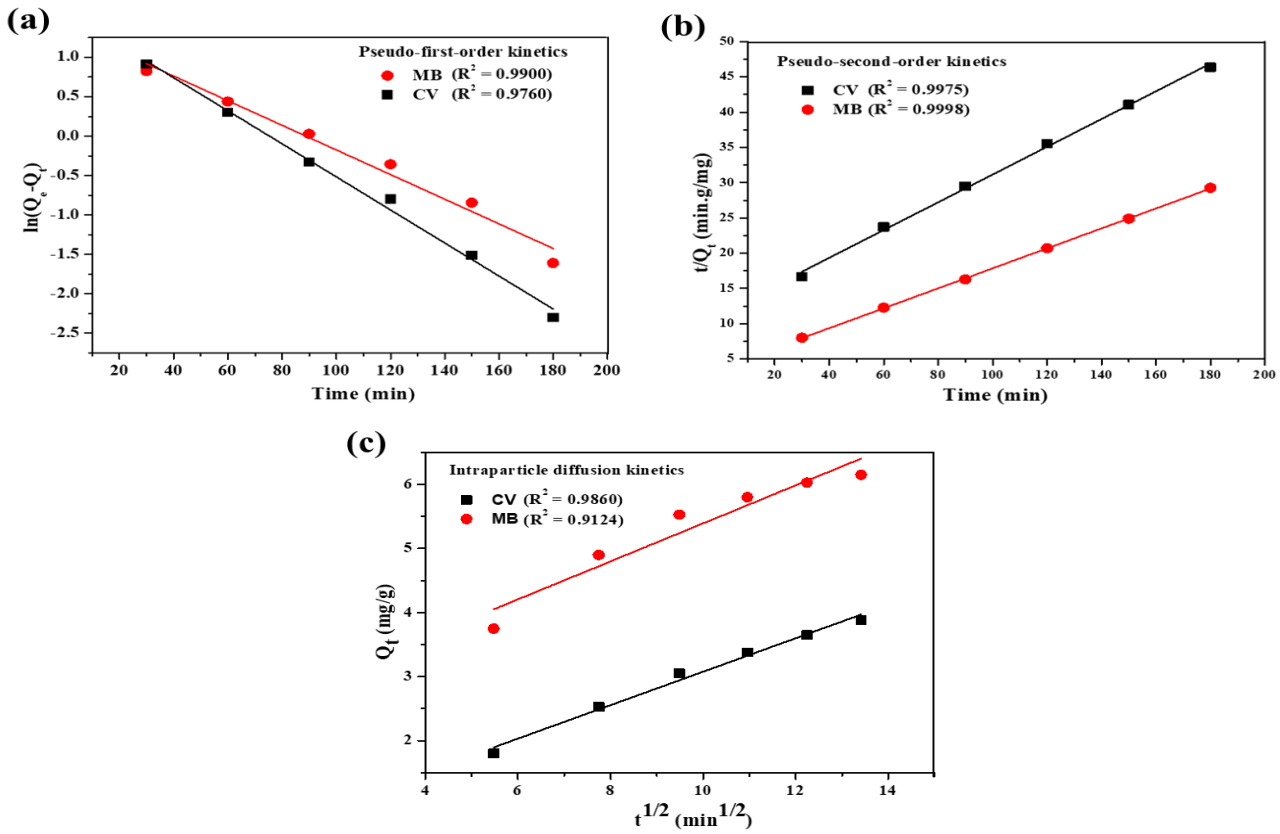

Fig. 8: Plot of linear fitting of pseudo-first-order kinetics model* (a), *pseudo-second-order kinetics model* (b), *and Intraparticle diffusion kinetics model* (c) *for CV and MB adsorption

Adsorption isotherms

Three adsorption isotherm models, Freundlich, Langmuir, and Temkin were used to determine the adsorption performance of MOF-801-100FA. Adsorption isotherm models were applied to get information about the mechanism of adsorption, evaluation of the performance of the adsorption process, and capacity of MOF-801-100FA as an adsorbent. Equations (3), (4), and (5) were used to represent these three adsorption isotherms. The isotherm data obtained for CV and MB dyes was fitted to the three models to determine the best fit for the adsorption data. Linear plots for Freundlich, Langmuir, and Temkin isotherms were shown in Fig. 7. The adsorption isotherm parameters for the three models were given in Table 3.

Based on the correlation coefficient (R^2) values, the Langmuir model (R^2 = 0.9939 for CV dye adsorption, and 0.9943 for MB dye adsorption) was the best fit compared to Freundlich (R^2 = 0.9913 for CV dye adsorption, and 0.9890 for MB dye adsorption) and Temkin (R^2 = 0.9811 for CV dye adsorption, and 0.9817 for MB dye adsorption) models.

The separation factor (R_L), an important characteristic of the Langmuir adsorption isotherm, was calculated using Equation (11):

$$R_L = \frac{1}{1+K_L C_o} \quad (11)$$

Here, C_o (mg/L) is the highest initial dye concentration and K_L is the Langmuir constant.

Table 4: Kinetic parameters for adsorption of CV and MB dyes on MOF-801-100 FA

Dye	C_o(mg/L)	$Q_{e,exp}$(mg/g)	Pseudo-first-order model			Pseudo-second-order model			Intraparticle diffusion model		
			$Q_{e,cal}$ (mg/g)	k_1(min^{-1})	R^2	$Q_{e,cal}$(mg/g)	k_2 (g/mg. min)	R^2	k_i (mg/g. $min^{1/2}$)	C	R^2
CV	5	4.08	4.003	0.0156	0.9760	5.08	0.00338	0.9975	0.2612	0.47	0.9860
MB	5	6.25	4.850	0.0210	0.9900	7.06	0.0054	0.9998	0.2965	2.42	0.9124

Table 5: Comparison with other MOF adsorbents for adsorption of CV and MB dyes

Dye	MOF adsorbent	Adsorption capacity (mg/g)	Reference
CV	MOF-801-100FA	18.90	Present work
	Fe-BDC	9.29	[34]
	$Cu_3(BTC)_2$	0.29	[37]
	H_2dtoaCu	165.83	[38]
	IFMC-2	2.40	[39]
	Cd-based	221.00	[40]
	Zn-based	54.50	[41]
	BUT-29	832.00	[42]
MB	MOF-801-100FA	30.40	Present work
	MIL-101(Fe)	58.82	[43]
	UiO-66-NO_2	41.70	[44]
	UiO-66-10%Ca	50.25	[45]
	MOF-235	187.00	[46]
	Fe-BDC MOF	8.65	[47]
	UiO-66	91.00	[48]
	ZIF-8	522.95	[49]

With the highest concentration of dye (50 mg/L) used in the adsorption experiment, the calculated value of R_L for CV was 0.303, and 0.246 for MB. The adsorption process was favorable as the obtained R_L values were between 0 and 1 [34]. From the linear plots of the Freundlich Isotherm model, the value of 1/n was found to be 0.497 for CV dye and 0.592 for MB dye. The obtained 1/n values indicate that the adsorbent applies to the entire CV and MB dye concentrations range. However, due to the small difference in R^2 values in Langmuir and Freundlich models, it is not clear whether adsorption occurred on a homogeneous or heterogeneous surface. The results obtained from linearized isotherm models are inconclusive. To overcome the limitations of the linearized models and to select the optimum adsorption isotherm model, nonlinear regression analysis must be applied [36].

Kinetics studies

Adsorption data were analyzed using three kinetic models, pseudo-first-order, pseudo-second-order, and intraparticle diffusion. These three models were represented by Equations (7), (8), and (9). The linear plots for the three models were presented in Fig. 8, and their corresponding kinetic parameters were listed in Table 4. Linear regression coefficient (R^2)

Values indicate that the pseudo-second-order kinetic model is the best fit for the adsorption data. The value of R^2 (0.9975 for CV dye adsorption, and 0.9998 for MB dye adsorption) for the pseudo-second-order kinetic plot is higher than the R^2 values of linear plots of the other two kinetics models. The pseudo-second-order rate constants were determined to be 3.378 x 10^{-3} g/mg min and 5.40 x 10^{-3} g/mg min for the adsorption of CV dye and MB dyes respectively. The results indicate that the adsorptive removal of CV and MB dyes from aqueous solution by MOF-801-100FA was due to chemisorption. The adsorption capacity of MOF-801-100FA for the adsorption of CV and MB dyes was compared with other MOF adsorbents as shown in Table 5.

Recyclability of adsorbent

To assess the recyclability of MOF-801-100FA, a desorption and regeneration experiment was conducted. A slight decrease in the adsorption capacity of MOF-801-100FA was observed with increasing cycle number. After five consecutive adsorption-desorption cycles, 81% of the initial MB dye removal efficiency and 74% of the initial CV dye removal efficiency was retained. The study shows that MOF-801-100FA has good recycling ability and could be used as a potential adsorbent for the removal of MB and CV dyes from aqueous solution.

CONCLUSIONS

In the present work, we demonstrated the energy-efficient and green *de novo* synthesis of defective MOF-801 samples using ultrasonication at room temperature. Among the four synthesized samples, MOF-801-100FA was highly crystalline with high specific surface area (BET area) of 699 m^2/g. TGA analysis revealed that the MOF-801-100FA sample was defective due to the missing linkers in the framework structure. The MOF was tested to remove two cationic dyes, CV and MB, from the aqueous solution by adsorption. The obtained adsorption data best fit the Langmuir and Freundlich isotherm models. Nonlinear regression analysis must be used to determine the optimum adsorption isotherm as the results obtained from linearized isotherm models are inconclusive. The adsorption kinetics was best described by the pseudo-second-order kinetics model. The MOF was found to have a higher adsorption efficiency toward MB dye. The maximum equilibrium adsorption capacity was 30.4 mg/g and 18.9 mg/g with MB and CV dyes having an initial concentration of 50 mg/L. The maximum adsorption of dyes was observed at a pH of 9. MOF-801-100FA was regenerated for the removal of CV and MB dyes with significant efficiency after five cycles. It is a promising adsorbent for the removal of these cationic dyes from aqueous solution.

Received : Dec.14, 2022 ; Accepted : Apr.17, 2023

REFERENCES

[1] Dutta S., Gupta B., Srivastava S.K., Gupta A.K., Recent Advances on the Removal of Dyes from Wastewater Using various Adsorbents: A Critical Review, *Materials Advances*, **21**: 4497-4531 (2021).

[2] Liang H., Hu X., Preparation of Magnetic Cellulose Nanocrystal- Modified Diatomite for Removal of Methylene Blue from Aqueous Solutions, *Iran. J. Chem. Chem. Eng. (IJCCE)*, **41(3)**: 787-798 (2022).

[3] Sakha P., Mahmoud Z., Tohid S.T., Mahdi K., Neural Network, Isotherm, and Kinetic Study for Wastewater Treatment Using Populus alba's Prund Material, *Iran. J. Chem. Chem. Eng. (IJCCE)*, **40(6)**: 1868-1881 (2021).

[4] Mohammad-Rezaei R., Khalilzadeh B., Rahimi F., Moradi S., Shahlaei M., Derakhshankhah H., Jaymand M., Simultaneous Removal of Cationic and Anionic Dyes from Simulated Industrial Effluents Using a Nature-Inspired Adsorbent, *Environ. Res.*, **214(3)**: 113966 (2022).

[5] Mohammad-Rezaei R., Khalilzadeh B., Rahimi F., Rezaee P., Arab S.S., Derakhshankhah H., Jaymand M., Simultaneous Removal of Cationic Dyes from Simulated Industrial Wastewater Using Sulfated Alginate Microparticles, *J. Mol. Liq.*, **363**: 119880 (2022).

[6] Beydaghdari M., Saboor F.H., Babapoor A., Karve V.V., Asgari M., Recent Advances in MOF-Based Adsorbents for Dye Removal from the Aquatic Environment, *Energies.*, **15(6)**: 2023 (2022).

[7] Fu M., Deng X., Wang S-Q., Yang F., Lin L-C., Zaworotko M.J., Dong Y., Scalable Robust Nano-Porous Zr-Based MOF Adsorbent with High-Capacity for Sustainable Water Purification, *Sep. Purif. Techno*., **288**: 120620 (2022).

[8] Au V.K-M., Recent Advances in the Use of Metal-Organic Frameworks for Dye Adsorption, *Front. Chem*., **8**: 70821 (2020).

[9] Xiang W., Zhang Y., Chen Y., Liu C-J., Tu X., Synthesis, Characterization, and Application of Defective Metal-Organic Frameworks: Current Status and Perspectives, *J. Mater. Chem. A*., **8**: 21526-21546 (2020).

[10] Choi J., Lin L-C., Grossman J.C., Role of Structural Defects in the Water Adsorption Properties of MOF-801, *J. Phys. Chem. C*., **122**: 5545-5552 (2018).

[11] Bai Y., Dou Y., Xie L-H, Rutledge W., Li J-R., Zhou H-C., Zr-Based Metal-Organic Frameworks: Design, Synthesis, Structure, and Applications, *Chem. Soc. Rev*., **45**: 2327-2367 (2016).

[12] Cao Y., Mi X., Li X., Wang B., Defect Engineering in Metal-Organic Frameworks as Futuristic Options for Purifica- Tion of Pollutants in an Aqueous Environment, *Front. Chem*., **9**: 673738 (2021).

[13] Wißmann G., Schaate A., Lilienthal S., Bremer I., Schneider A.M., Behrens P., Modulated Synthesis of Zr-Fumarate MOF, *Microporous Mesoporous Mater*., **152**: 64-70 (2012).

[14] Butova V.V., Pankin I.A., Burachevskaya O.A., Vetlitsyna-Novikova K.S., Soldatov A.V., New Fast Synthesis of MOF-801 for Water and Hydrogen Storage: Modulator Effect and Recycling Options, *Inorganica Chimica Acta*., **514**: 120025 (2021).

[15] Kim H., Yang S., Rao S.R., Narayanan S., Kapustin E.A., Furukawa H., Umans A.S., Yaghi O.M., Wang E.N., Water Harvesting from Air with Metal-Organic Frameworks Powered by Natural Sunlight, *Science*, **356**: 430-434 (2017).

[16] Saidi M., Benomara A., Mokhtari M., Boukli-Hacene L., Sonochemical Synthesis of Zr-fumaric Based Metal-Organic Framework (MOF) and Its Performance Evaluation in Methyl Violet 2B Decolorization by Photocatalysis, *React Kinet Mech Catal*., **131**: 1009-1021 (2020).

[17] Ke F., Peng C., Zhang T., Zhang M., Zhou C., Cai H., Zhu J., Wan X., Fumarate-Based Metal-Organic Frameworks as a New Platform for Highly Selective Removal of Fluoride from Brick Tea, *Sci Rep*., **8**: 939 (2018).

[18] Prabhu S.M., Srinivasarao K., Park C.M., Sasaki. K., Synthesis of Modulator-Driven Highly Stable Zirconium- Fumarate Frameworks and Mechanistic Investigations of their Arsenite and Arsenate Adsorption from Aqueous Solutions, *Cryst. Eng. Comm*., **21**: 2320-2332 (2019).

[19] Yoo J., Ryu U., Kwon W., Choi K.M., A Multi-Dye Containing MOF for the Ratiometric Detection and Simultaneous Removal of $Cr_2O_7^{2-}$ in the Presence of Interfering Ions, *Sens Actuators B: Chem*., **283**: 426-433 (2019).

[20] Zheng M., Zhao X., Wang K., She Y., Gao Z., Highly Efficient Removal of Cr(VI) on a Stable Metal-Organic Framework Based on Enhanced H-Bond Interaction, *Ind. Eng. Chem. Res*., **58**: 23330-23337 (2019).

[21] Lázaro I.A., Haddad S., Rodrigo-Muñoz J.M., , Forgan R.S., Surface-Functionalization of Zr-Fumarate MOF for Selective Cytotoxicity and Immune System Compatibility in Nanoscale Drug Delivery, *ACS Appl. Mater. Interfaces*., **10**: 31146-3115 (2018).

[22] Lacomi P., Formalik F., Marreiros J., Shang J., Justyna R., Mohmeyer A., Behrens P., Ameloot R., Kuchta B., Llewellyn P.L., Role of Structural Defects in the Adsorption and Separation of C3 Hydrocarbons in Zr-Fumarate- MOF (MOF-801), *Chem. Mater*., **31**: 8413-8423 (2019).

[23] Rouhani M., Ramazani A., Joo S.W., Novel, Fast and Efficient One-Pot Sonochemical Synthesis of 2-Aryl-1,3,4- Oxadiazoles, *Ultrason Sonochem*., **21(1)**: 262-267 (2014).

[24] Rouhani M., Ramazani A., Joo S.W., Ultrasonics in Isocyanide-Based Multicomponent Reactions: A New, Efficient and Fast Method for the Synthesis of Fully Substituted 1,3,4-Oxadiazole Derivatives under Ultrasound Irradiation, *Ultrason Sonochem*., **22**: 391-396 (2014).

[25] Ramazani A., Rouhani M., Joo S.W., Catalyst-Free Sonosynthesis of Highly Substituted Propenamide Derivatives in Water, *Ultrason Sonochem*., **28**: 393-399 (2016).

[26] Qiu L-G., Li Z-Q., Wu Y., Wang W., Xu T., Jiang X., Facile Synthesis of Nanocrystals of Microporous Metal-Organic Framework by an Ultrasonic Method and Selective Sensing of Organoamines, *Chem. Comm*., **31**: 3642-3644 (2008).

[27] Jahan I., Rupam T.H., Palash M.L., Rocky K.A., Saha B.B., Energy Efficient Green Synthesized MOF-801 for Adsorption Cooling Applications, *J. Mol. Liq*., **345**: 117760 (2022).

[28] Mani S., Bhargava R.N., Exposure to Crystal Violet, Its Toxic, Genotoxic and Carcinogenic Effects on Environment and Its Degradation and Detoxification for Environmental Safety, *Rev. Environ. Contam. Toxicol*., **237**: 71-104 (2016).

[29] Khan I., Saeed K., Zekker I., Zhang B., Hendi A.H., Ahmad A., Ahmad S., Zada N., Ahmad H., Shah L.A., Shah T., Khan I., Review on Methylene Blue: Its Properties, Uses, Toxicity and Photodegradation, *Water* **14**: 242 (2022).

[30] Furukawa H., Gándara F., Zhang Y-B., Jian J., Queen W.L., Hudson M.R., Yaghi O.M., Water Adsorption in Porous Metal-Organic Frameworks and Related Materials, *J Am. Chem Soc*., **136**: 4369-4381 (2014).

[31] Ren J., Musyoka N.M., Langmi H.W., North B.C., Mathe M., Pang W., Wang M., Walker J., In-Situ IR Monitoring of the Formation of Zr-Fumarate MOF, *Appl. Surf Sci*., **404**: 263-267 (2017).

[32] Prasetya N., Li K., Synthesis of Defective MOF-801 *via* an Environmentally Benign Approach for Diclofenac Removal from Water, *Sep. Purif. Techno*., **301**: 122024 (2022).

[33] Shearer G.C., Chavan S., Bordiga S., Svelle S., Olsbye U., Lillerud K.P., Defect Engineering: Tuning the Porosity and Composition of the Metal-Organic Framework UiO-66, *Chem. Mater*., **28**: 3749-3761 (2016).

[34] Soni S., Bajpai P.K., Bharti D., Mittal J., Arora C., Removal of Crystal Violet from Aqueous Solution Using Iron Based Metal Organic Framework, *Desalination Water Treat*., **205**: 386-399 (2020).

[35] Khan M.S., Khalid M., Shahid M., What Triggers Dye Adsorption by Metal Organic Frameworks? The Current Perspectives, *Mater. Adv*., **1**: 1575-1601 (2020).

[36] Tonk S., Rápó E., Linear and Nonlinear Regression Analysis for the Adsorption of Remazol Dye by Romanian Brewery Waste By-Product, Saccharomyces Cerevisiae, *Int. J. Mol. Sci*., **23(19)**: 11827 (2022).

[37] Loera-Serna S., Garcia-Ortiz J., Ortiz E., Dyes Adsorption on $Cu_3(BTC)_2$ Metal-Organic Framework. Advanced Materials, *TechConnect Briefs*, **1**: 331-334 (2016).

[38] Li X., Zheng L., Huang L., Zheng O., Lin Z., Guo L., Qiu B., Chen G., Adsorption Removal of Crystal Violet from Solution Using a Metal-Organic Frameworks Material, Copper Coordination Polymer with Dithiooxamide, *J. Appl. Polym. Sci*., **129**: 2857-2864 (2013).

[39] Qin J-S., Zhang S-R., Du D-Y., Shen P., Bao S-J., Lan Y-Q., Su Z-M., A Microporous An-ionic Metal-Organic Framework for Sensing Luminescence of Lanthanide (III) Ions and Selective Absorption of Dyes by Ionic Exchange, *Chem. Eur. J*., **20**: 5625-5630 (2014).

[40] Chand S., Elahi S.M., Pal A., Das M.C., A New Set of Cd(II)-coordination Polymers with Mixed Ligand of Dicarboxy- Late and Pyridyl Substituted Diaminotriazine: Selective Sorption Towards CO_2 and Cationic Dye, *Dalton Trans*., **46**: 9901-9911 (2017).

[41] Zhang J., Li F., Sun Q., Rapid and Selective Adsorption of Cationic Dyes by a Unique Metal-Organic Framework with Decorated Pore Surface, *Appl. Surf. Sci*., **440**: 1219-1226 (2018).

[42] Yang Q., Wang B., Chen Y., Xie Y., An Anionic In(III)-Based Metal-Organic Framework with Lewis Basic Sites for the Selective Adsorption and Separation of Organic Cationic Dyes, *Chin. Chem. Lett*., **30**: 234-238 (2019).

[43] Eltaweil A.S., El-Monaem E.M., Omer A.M, Khalifa R.E., El-Latif, M.M.A., El-Subruiti G.M., Efficient Removal of Toxic Methylene blue (MB) dye from Aqueous Solution Using a Metal-Organic Framework (MOF) MIL-101(Fe): Isotherms, Kinetics, and Thermodynamic Studies, *Desalination Water Treat.*, **189**: 395-407 (2020).

[44] Dinh H.T., Tran N.T., Trinh D.X., Investigation into the Adsorption of Methylene Blue and Methyl Orange by UiO-66-NO_2 Nanoparticles, *J. Anal. Methods Chem*., **2021**: 1-10 (2021).

[45] Amery N.Al., Abid H.R., Wang S., Liu S., Removal of Methylene Blue (MB) by Bimetallic Metal Organic Framework Framework, *J. Appl. Mat. and Tech*., **2**: 36-49 (2020).

[46] Haque E., Jun W.J., Jhung S.H., Adsorptive Removal of Methyl Orange and Methylene Blue from Aqueous Solution with a Metal-Organic Framework Material, Iron Terephthalate, *J. Hazard Mater*., **185**: 507-511 (2011).

[47] Arora C., Soni S., Sahu S., Mittal J., Kumar P., Bajpai P.K., Iron Based Metal Organic Framework for Efficient Removal of Methylene Blue dye from Industrial Waste, *J. Mol. Liq*., **284**: 343-352 (2019).

[48] Mohammadi A.A., Alinejad A., Kamarehie B., Javan S., Ghaderpoury A., Ahmadpour M., Ghaderpoori M., Metal- Organic Framework Uio-66 for Adsorption of Methylene Blue dye from Aqueous Solutions, *Int. J. Environ. Sci. Technol*., **14**: 1959-1968 (2017).

[49] Al-Wasidi A.S., Alzahrani I.I.S., Naglah A.M., El-Desouky M.G., Khalil M.A., El-Bindary A.A., El-Bindary M.A., Effective Removal of Methylene Blue From Aqueous Solution and Using Metal-Organic Framework; Modeling Analysis, Statistical Physics Treatment DFT Calculations, *Chemistry Select*, **6**: 11431-11447 (2021).